

Two-Step Growth of MgO Films on Sapphire (0001) Substrates by Radio Frequency Plasma-Assisted Molecular Beam Epitaxy *

MEI Zeng-Xia(梅增霞), DU Xiao-Long(杜小龙)**, ZENG Zhao-Quan(曾兆权), GUO Yang(郭阳),
WANG Jian(王健), JIA Jin-Feng(贾金锋), XUE Qi-Kun(薛其坤)

State Key Laboratory for Surface Science, Institute of Physics, Chinese Academy of Sciences, Beijing 100080

(Received 26 June 2003)

We report on the growth of rock salt MgO films on sapphire (0001) substrates by rf plasma-assisted molecular beam epitaxy. A two-step method, i.e. high temperature epilayer growth after low-temperature buffer layer growth, was adopted to obtain the single crystal MgO film. The epitaxial orientation between the MgO epilayer and the sapphire (0001) substrate was studied by using in situ reflection high energy electron diffraction and ex situ x-ray diffraction, and it is found that the MgO film grows with [111] orientation. The role of the low temperature buffer layer in the improvement of crystal quality of the MgO epilayer is discussed based on the cross-sectional scanning electron microscopy.

PACS: 81.15.Hi, 68.55.-a

Rock salt MgO plays an important role in band gap engineering due to its huge band gap of 7.8 eV.^[1,2] In terms of band structure tailoring, it can be alloyed with ZnO, another II-VI wide-band-gap (3.37 eV) semiconductor, for many applications in optical and electronic devices, such as solar cells, transparent conductors for displays, light emitters, sensors, varistors, modulators, and UV detectors.^[3] MgZnO was found to be of the wurtzite structure when the Mg content is less than 30%,^[4] whereas cubic MgZnO was formed with the Zn content less than 25%.^[5] In the former case, a portion of Zn atoms in the wurtzite ZnO lattice is replaced by Mg atoms, while in the latter case, some Mg atoms in the rock salt MgO lattices are substituted by Zn atoms. It is of great importance to develop an epitaxy technique for MgO in order to obtain high quality and high Zn content MgZnO with a cubic structure.

The low-temperature (LT) buffer technique has been known as a successful solution for preparing high-quality epitaxial films in highly mismatched systems, such as ZnO^[6-8] and GaN^[9] on sapphire (0001). It was demonstrated that an LT buffer layer can effectively relax strain and can reduce the defect density caused by large lattice mismatch, which facilitates the following homoepitaxial growth at high temperatures. In this Letter, based on the same idea we employ a two-step method to prepare single crystal MgO films on sapphire (0001) by using rf plasma-assisted molecular beam epitaxy (MBE). A thin MgO buffer layer is deposited at low temperature prior to growth of the MgO epilayer at high temperature. The epitaxial orientation between the MgO epilayer and the sapphire substrate is established using in situ reflection high

energy electron diffraction (RHEED) observation and ex situ x-ray diffraction (XRD) measurement. Based on the cross-sectional scanning electron microscopy (SEM) observations, we also study the role of the low-temperature buffer layer in the improvement of crystal quality of the MgO epilayer.

The MgO samples were grown on the sapphire (0001) using an rf plasma-assisted MBE system which was modified from a conventional MBE system (MBE-IV, ShenYang KeYi). The base pressure in the growth chamber was $\sim 9 \times 10^{-10}$ Torr. Magnesium was supplied by evaporating 99.95% elemental Mg from a commercial Knudsen cell. Active oxygen radicals were produced by the rf-plasma system (HD25R, Oxford Applied Research). The flow rate of oxygen gas was controlled by a mass flow controller. High energy ions were removed by using a dc bias on two plates in front of the discharge tube.

After being degreased in trichloroethylene and methanol, the sapphire substrates were chemically etched for 30 min in a hot solution of H₂SO₄:H₃PO₄=3:1 at 110°C to remove the surface contamination and the damaged surface layers by mechanical polishing. The substrates were exposed to the oxygen radicals for 30 min at 450°C after thermal cleaning at 800°C for 30 min. Then, the two-step growth process of the MgO film was performed, i.e. the LT buffer layer growth at 450°C and the high-temperature (HT) epilayer growth at 650°C. The evolution of the surface morphology and crystallinity was monitored by RHEED. The crystal quality and in-plane orientation of the MgO films were characterized using an x-ray diffractometer (Bede D1, Bede Scientific Instruments Ltd., UK). In addition, a field

* Supported by the National Natural Science Foundation of China under Grant Nos 60376004, 10174089, and 60021403, and the National Key Basic Research and Development Programme of China under Grant No 2002CB613502.

** Email: To whom correspondence should be addressed. E-mail: xldu@aphy.iphy.ac.cn

emission (FE) scanning electron microscope (XL 30 S-FEG, FEI Co., Holland) was used to examine the cross-section morphology of the MgO samples.

Typical Stranski–Krastanov mode was observed during the growth of the MgO buffer layer. Figure 1 shows the RHEED patterns at different stages of the MgO buffer layer deposition. A sharp streaky pattern of the Al_2O_3 substrate was observed after oxygen radical exposure [Fig. 1(a)]. This pattern changes into a diffuse streaky one [Fig. 1(b)] when the deposition of the MgO buffer layer begins at 450°C . The streaky patterns suggest an initial 2D nucleation, which cor-

responds most likely to the wetting by MgO of the oxygen-terminated sapphire (0001) surface after the oxygen radical exposure. Further growth of MgO leads to diffuse spotty patterns, indicating the formation of 3D islands on the wetting layer due to the serious lattice mismatch (7.8%) between MgO and sapphire substrate. Figure 1(c) shows an RHEED pattern of the as-grown MgO buffer layer. The RHEED patterns [Fig. 1(d)] become streaky again after buffer layer annealing at 750°C for 10 min, which is attributed to the re-crystallization and coalescence of the 3D MgO islands. The sixfold symmetry and the

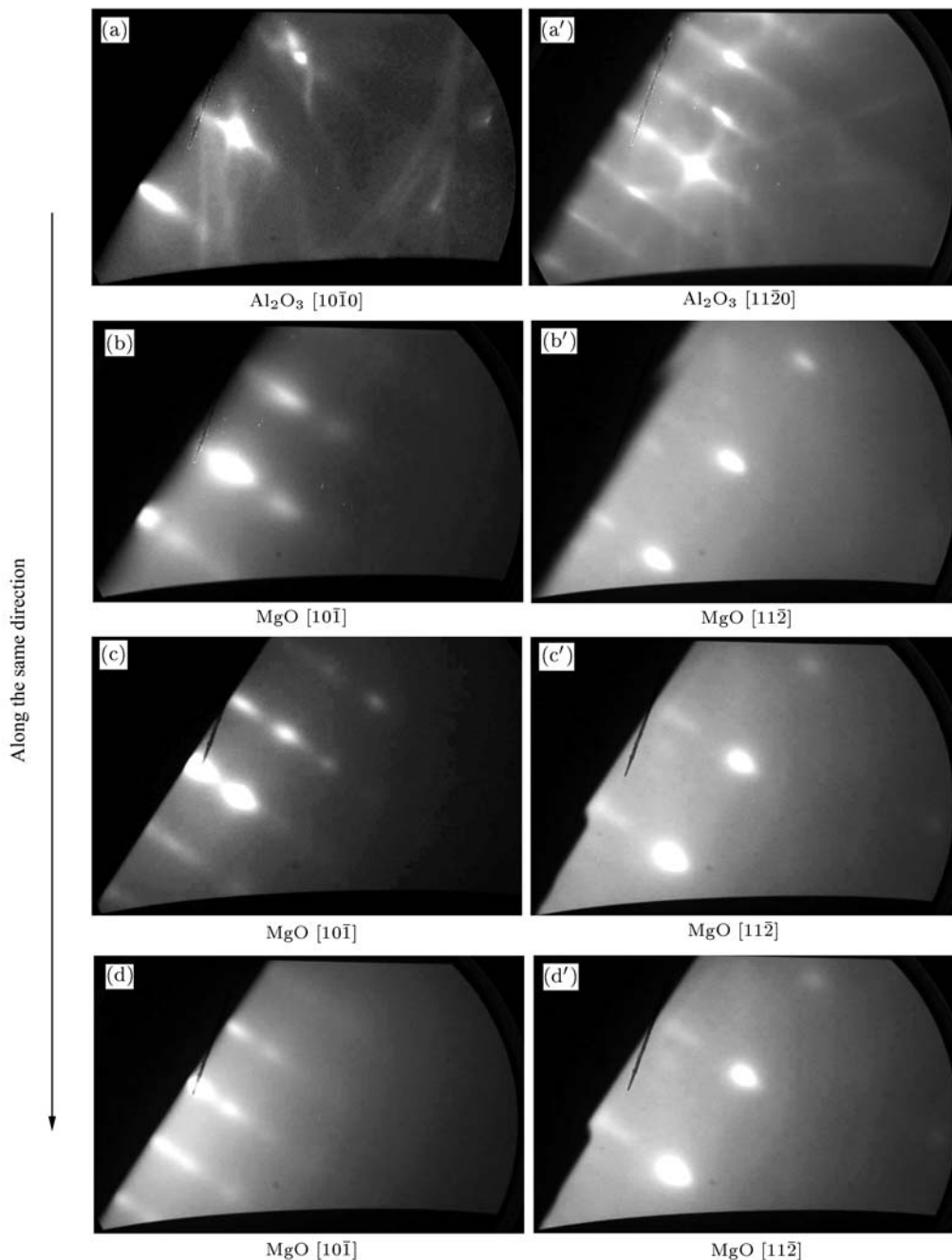


Fig. 1. RHEED patterns during the growth of MgO buffer on sapphire substrate: (a) Al_2O_3 (0001) surface after the oxygen radical exposure, (b) initial growth stage of MgO buffer, (c) as-grown MgO buffer, (d) MgO buffer layer after annealing.

rod spacing of the pattern of Fig. 1(d) indicate that rock salt MgO grows with the [111] orientation. The epitaxial orientation between Al_2O_3 (0001) and MgO is MgO $[10\bar{1}]//\text{Al}_2\text{O}_3$ $[10\bar{1}0]$ and MgO $[11\bar{2}]/\text{Al}_2\text{O}_3$ $[11\bar{2}0]$. This relationship is further confirmed by the XRD measurement, which will be discussed in the following. The MgO epilayer growth begins when the substrate temperature ramps to 650°C . The RHEED pattern remains almost unchanged during the growth of MgO epilayer (not shown).

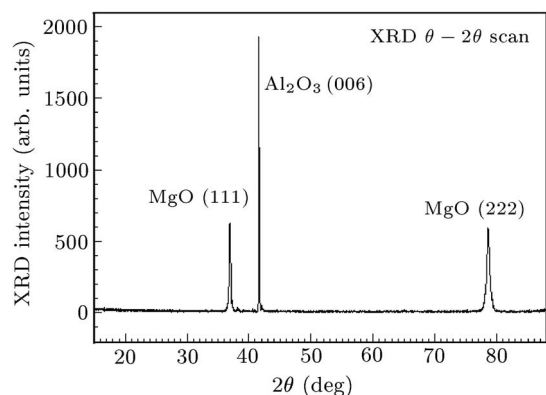


Fig. 2. XRD scan of the MgO film grown on sapphire substrate. Three peaks at $2\theta = 36.9^\circ$, 41.7° and 78.5° are originated from MgO(111), sapphire substrate (0006), and MgO(222).

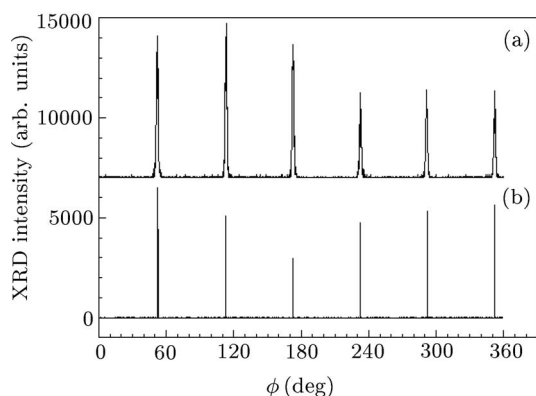


Fig. 3. XRD ϕ -scans of (a) MgO (220) and (b) sapphire substrate (1123). The epitaxial orientation is MgO $[10\bar{1}]//\text{Al}_2\text{O}_3$ $[10\bar{1}0]$ and MgO $[11\bar{2}]/\text{Al}_2\text{O}_3$ $[11\bar{2}0]$.

Figure 2 shows the XRD $\theta - 2\theta$ scan curve of the MgO film. Three peaks are observed at $2\theta = 36.9^\circ$, 41.7° and 78.5° , which correspond to the diffractions from MgO (111), sapphire substrate (0006), and MgO (222), respectively. The FWHM of the MgO (111) diffraction peak is 0.26° . The above results indicate a high quality single crystal MgO film and the remarkable effect of this thin MgO buffer layer on improving the crystal quality. Figure 3 shows the XRD ϕ -scans of the MgO (220) and sapphire substrate (1123). We obtained six peaks for both the MgO film and the sap-

phire substrate, respectively. The relative peak position between MgO (220) and sapphire (1123) agrees with the epitaxial orientation as observed in RHEED.

In order to investigate the role of the MgO buffer, we carried out a cross-sectional SEM observation. Figure 4(a) shows the cross-sectional SEM image of the MgO sample grown with the two-step growth process. The evolution of the sub-grain structure in the MgO film is illustrated with the cleaving stripes.

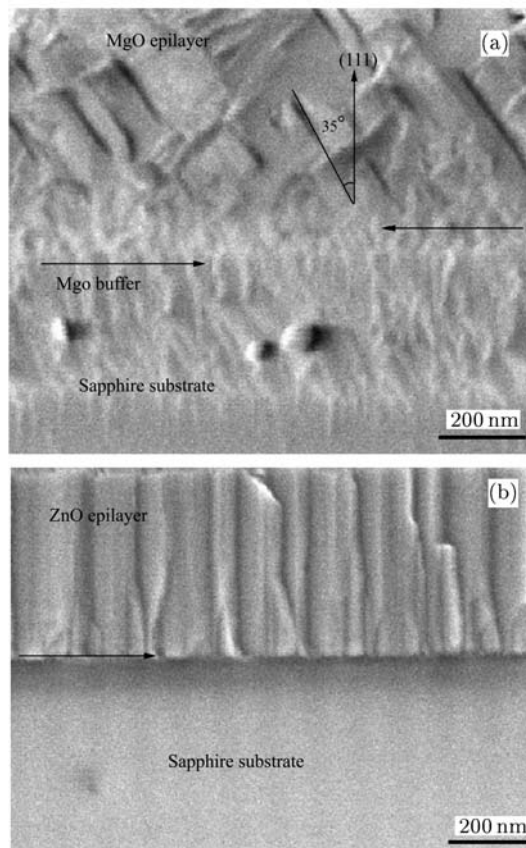


Fig. 4. Cross-sectional SEM images of the MgO sample (a) and the ZnO sample (b) grown on the sapphire substrates, illustrating distinct sub-grain structures.

In contrast to the well-known mosaic structure [Fig. 4(b)] of the wurtzite ZnO film on the sapphire (0001) substrate, quite different sub-grain structure is observed in the MgO film as shown in Fig. 4(a). Many parallel cleave stripes are observed in the MgO film. These cleave stripes originate from the grain boundaries which lie in the (100) plane. They tilt 35° with respect to the [111] direction of MgO, which is well consistent with the 55° angle between $\{100\}$ planes and the (111) surface.^[10,11] It is well-known that two of the lowest index $\{100\}$ and $\{110\}$ surfaces of oxides with rock-salt structure are neutral, whereas the (111) type surfaces are polar. The polar (111) surface has diverging surface energy which can be lowered to the smallest finite value if the polar surfaces facet into neutral $\{100\}$ faces or form reconstructions.^[12–14] Thus,

it is a significant issue to understand the stabilization process of MgO (111) surface during the epitaxial growth. In our case, no surface reconstruction was observed on the MgO(111) plane by RHEED during the growth. In order to reduce the surface energy, the MgO film tends to form a sub-grain structure along the [100] direction, even though the MgO film grows along the [111] direction.

Figure 4(a) also illustrates that the grain size in the MgO epilayer is much larger than that in the buffer layer. In the as-grown buffer layer, the small 3D islands are a few tens of nanometres in size, and will coalesce into larger ones during annealing. As the annealed buffer layer serves as a template for MgO epilayer growth at HT, the grains of a few hundreds of nanometres observed in the MgO epilayer must be closely related to the island coalescence.

In summary, single crystal MgO film was deposited on the sapphire (0001) substrate by rf plasma-assisted MBE using a two-step method. The MgO film is [111] oriented, and the epitaxial orientation is determined to be MgO $[10\bar{1}]//\text{Al}_2\text{O}_3 [10\bar{1}0]$ and MgO $[11\bar{2}]//\text{Al}_2\text{O}_3 [11\bar{2}0]$. Typical Stranski–Krastanov mode is observed during growth of the MgO buffer layer. The small islands in the as-grown buffer become much larger and their crystal quality is greatly improved after annealing, which are confirmed by in situ RHEED observation and ex situ XRD and SEM measurements.

The authors would like to thank Jun-Ming Zhou and Hong Chen for fruitful discussion and technical assistance.

References

- [1] Choopun S, Vispute R D, Yang W, Sharma R P, Venkatesan T and Shen H 2002 *Appl. Phys. Lett.* **80** 1529
- [2] Ueda A, Mu R, Tung Y -S, Wu M H, Zavalin A, Wang P W and Henderson D O 2001 *J. Phys.: Condens. Matter* **13** 5535
- [3] Look D C 2001 *Mater. Sci. Engin. B* **80** 383
- [4] Ohtomo A, Kawasaki M, Koida T, Masubuchi K, Koinuma H, Sakurai Y, Yoshida Y, Yasuda T and Segawa Y 1998 *Appl. Phys. Lett.* **72** 2466
- [5] Qiu D J et al, Wu H Z, Chen N B and Xu T N 2003 *Chin. Phys. Lett.* **20** 582
- [6] Wang X Q, Iwaki H, Murakami M, Du X L, Ishitani Y and Yoshikawa A 2003 *Jpn. J. Appl. Phys.* **42** L99
- [7] Chen Y F, Ko H-J, Hong S -K and Yao T 2000 *Appl. Phys. Lett.* **76** 559
- [8] Iwata K, Fons P, Niki S, Yamada A, Matsubara K, Nakahara K and Takasu H 2000 *Phys. Status Solidi A* **180** 287
- [9] Strite S and Morkoc H 1992 *J. Vac. Sci. Technol. B* **10** 1237 and references therein
- [10] Gajdardziska-Josifovska M et al, Plass R, Schofield M A, Giese D R and Sharma R 2002 *J. Electron Microsc.* **51** S13
- [11] Plass R, Feller J and Gajdardziska-Josifovska M 1998 *Surf. Sci.* **414** 26
- [12] Henrich V E 1976 *Surf. Sci.* **57** 385
- [13] Gajdardziska-Josifovska M, Crozier P A and Cowley J M 1991 *Surf. Sci. Lett.* **248** L259
- [14] Barbier A, Mocuta C, Kuhlbeck H, Peters K F, Richter B and Renaud G 2000 *Phys. Rev. Lett.* **84** 2897